doi:10.1038/nature10617

Supplementary Methods

GROTTA DEL CAVALLO

Description of the site and history of excavations

Grotta del Cavallo (40°9'18.85"N, 17° 57' 37.27"E) is situated on the rocky coast of the Bay of Uluzzo, Nardò, around 90 km south of the town of Taranto in Apulia, SE Italy. It is located within a low Mesozoic limestone plateau, about 15m above the present day shore, with a large, 5 m wide by 2.5 m high opening facing NW and an approximately circular shape, about 9 m in diameter[31]. Cavallo was discovered in 1960 and was initially investigated in 1961 by A. Palma di Cesnola. Official excavations took place between 1963–1966[31-34], and again between 1986–2008 focusing on the Mousterian parts of the sequence[35,36]. In the interlude between the two series of excavations, looters severely disturbed the central part of the deposits, removing much of the Upper Palaeolithic layers. In the light of this damage, salvage excavations were conducted by the University of Siena (P. Gambassini and colleagues) for four seasons in the late 1970s/early 1980s and a metal gate was installed at the entrance of the cave. In the process of installing it, the standing sections were cleaned and some free-standing deposits at the entrance of the cave were carefully removed and correlated to the original stratigraphy.

Stratigraphy

The site preserves a long stratigraphic succession comprising about 7 m of archaeological deposits directly based on a marine interglacial beach conglomerate (layer N) (Fig. S1). The archaeological sequence of Cavallo is dominated by Middle Palaeolithic layers (MIV-F I),

capped by a thin layer of green volcanic ash (Fα), which separates Mousterian from the overlying Uluzzian layers (E-DIb) (Fig. S1).

The Uluzzian deposits, about 80-85 cm thick, were excavated both in the 1960s and in the late 1970s/early 1980s at separate sections of the site. A correlation is given in Table S1.

These layers are divided into Archaic Uluzzian (E III), Evolved Uluzzian (EII-I) and Final Uluzzian (D II – D Ib)[37-40]. They are separated from the upper part of the sequence by a stalagmitic crust (D Ia) and two sterile layers of volcanic ash (C II and C Ia-b). The tephra in layer C has been traditionally assigned to the Campanian Ignimbrite eruption[41] on empirical grounds and by comparison to other sequences (e.g. Castelcivita), but no geochemical characterisation has been attempted. Directly superimposed are Epigravettian horizons B II- B I (Romanellian and Epiromanellian *facies*), of much younger age (≈11,000 yr BP).

The Uluzzian layers of Cavallo comprise the most complete stratified sequence of the technocomplex ever revealed.

DENTAL MORPHOMETRIC ANALYSIS

Comparative sample

Table S2 shows the comparative sample used for the morphometric analyses. The whole corpus, except for the UPMH specimen Brillenhöhle, was used for outline analysis. For enamel thickness and dental tissue proportions, only individuals with wear stage equal or lower than 3 (based on Smith[42]) were selected. Nonetheless, the different wear stage of the fossil sample forced us to follow different solutions for dM^1 and dM^2. The fossil dM^1 sample is almost completely dominated by wear stage 3. Accordingly, a modern human comparative sample of similar wear stage was created. Additionally, since Cavallo-B is unworn, we

collected also an unworn modern human sample to figure out the hypothetical 2D AET and 2D RET indexes that Cavallo-B could have in wear stage 3. For the dM^2 Neanderthal sample, because almost all individuals are unworn or slightly worn, specimens with wear stage 3 were not considered to measure the enamel thickness and dental tissue proportions. Conversely, in the modern human sample specimens with wear stage 3 were included to create the worst scenario in support to the attribution of Cavallo specimen to *H. sapiens*. Namely, the AET and RET indexes obtained for the modern human sample are slightly underestimated.

Scanning of the specimens and segmentation

The original specimens used in this study were scanned at the Vienna Micro-CT Lab, Department of Anthropology, University of Vienna (Viscom X8060 µCT scanner using the following scan parameters: 130kV, 100mA, isotropic voxel size=25µm), at the Paleoanthropology High Resolution CT laboratory, Senckenberg Center for Human Evolution and Paleoecology, Eberhard Karls Universität Tübingen (v|tome|x s 240 µCT from GE Pheonix, using the following scan parameters: 130kV, 100mA, isotropic voxel size ranging from=15-26µm), and at the AST-RX platform (Accès Scientifique à la Tomographie à Rayons X) at the Muséum national d'Histoire naturelle (using the following scan parameters:150 kV, 220 mA, isotropic voxel size=33.62µm). Details about the scanning procedure of the other specimens can be found in NESPOS (Neanderthal Studies Professional Online Service) Database 2011.

For the segmentation process, the half-maximum height (HMH) protocol[43] was used to reconstruct 3D digital surface models for the dentine and the enamel of each CT-scanned tooth using the software package Amira 5.3 (Mercury Computer Systems, Chelmsford, MA). This protocol samples the Hounsfield values on either side of the transition between two

adjacent tissues and takes the value halfway between them as the threshold value. When voxels were located on the boundary between two tissues with similar Hounsfield values and the automatic threshold could not distinguish the differences (for example, for the presence of cracks or small decays), manual corrections were conducted.

Digital reconstruction of Engis 2 dM^1 crown outline

Computer-Aided Design (CAD) techniques in RapidForm XOR2 (INUS Technology, Inc.) were used to restore the dM^1 crown outline of the Neanderthal specimen Engis 2 (Fig. S2; the reconstructed regions in red). At the distal side, the small part of the outline missing was reconstructed by using a spline (namely, a curve interpolation). At the buccal side, the enamel is chipped away due to a post-mortem fracture, which reveals the dentine. This missing region of the enamel outline was restored virtually by offset of the corresponding dentine outline. In particular, the dentine outline exposed was duplicated and translated towards the enamel outline of 0.39 mm (length equal to the enamel thickness measured in the fracture). Finally, that segment was fused to the rest of the outline.

Statistical analysis

The data was analyzed via software routines written in R[44]. Table S3 shows the complete descriptive statistic for dM^1 and dM^2 enamel thickness and dental tissue proportions.

Principal Component Analysis (PCA)

The PCA of the matrix of Procrustes coordinates was carried out on the sample of the dM^1 crown and the dM^2 cervical outlines respectively. We applied Anderson's formula to test the

deviation from joint equality of any sequence of consecutive eigenvalues[45,46]. When the formula is applied to a single pair of consecutive eigenvalues, it states that the distribution of $2N \log(a/g)$ is that of an ordinary chi-square on two degrees of freedom. Here N is the sample size (Cavallo's teeth excluded), a is the arithmetic mean of the pair of consecutive eigenvalues, and g is the geometric mean of this same pair of eigenvalues. The expected value of the chi-square is two (its degrees of freedom), and so no PC (eigenvector) should be considered for interpretation if, when its eigenvalue is compared with the next eigenvalue, $2N \log(a/g)$ does not exceed two, as their ordination most probably accounts only for noise.

PCA of the dM^1 and dM^2 outlines

When applying Anderson's formula[45] to test PC2 and PC3 from the PCA of the dM^1s, of eigenvalues of 0.083 and 0.072, we obtain the value of 0.644 (N =32) — clearly below the expected value of a chi-square on two degree of freedom. Likewise for the PCA of the dM^2s, PC3 and PC4, of eigenvalues 0.083 and 0.070, Anderson's value is equal to 1.097 (N =38). The eigenvalues of PC2 and PC3 from the PCA of the dM^1s and those of PC3 and PC4 from the PCA of the dM^2s are nearly equal, and hence cannot be considered for either interpretation or further statistical analyses.

Quadratic Discriminant Analysis (QDA)

The leave-one-out cross-validation QDA was used for the taxonomic classification of Cavallo-B and Cavallo-C. We built up QDA models on RET, AET and subsets of PCs of the outline analysis, leaving out the data from the Cavallo specimens. The use of QDA is justified as the results show that the variances of the dental variables are significantly different between Neanderthals and modern humans. The computation of the posterior probabilities (P_{post}) was made with an equal prior probability ($P_{prior} = 0.5$) for the Neanderthal and modern

human groups (UPMH+RMH). Taxonomic determination is accepted with a P_{post} equal or superior to 0.90. The performance of the QDA models is defined by the percentage of specimens which taxon is determined with a $P_{post} \geq 0.90$ (correctly and incorrectly classified) and by the percentage of specimens correctly classified (accuracy). Cavallo's teeth have been tested through all the iterations of leave-one-out cross-validation QDAs. The accuracy of the classification was also computed as the number of iterations for which Cavallo's teeth were classified with a $P_{post} \geq 0.90$ either as modern human or Neanderthal.

QDA of dM^1 and dM^2 PCs, RET and AET

Table S4 summarizes the analysis. The performance of the QDA models is high for the tooth outlines (dM^1: PC1 scores, dM^2: PC1 and PC2 scores) and RET with a high accuracy ranging from 96.3% to 100% and percentage of specimens classified superior to 82%. For both dM^1 and dM^2, although the accuracy is high, the QDA models based on AET have a low power of classification when the threshold of decision $P_{post} \geq 0.90$. Therefore, they are not used for the classification of Cavallo-B and Cavallo-C. According to the QDA models based on outline and RET data, Cavallo-B and Cavallo-C are classified as modern humans with a $P_{post} > 0.90$ and with an accuracy of 100%.

RADIOCARBON DATING

Previous chronology

Since the first identification of the technocomplex in 1963 by Palma di Cesnola[33,34] and for four decades afterwards, the chronology of the Uluzzian of Cavallo was based on an infinite conventional radiocarbon date, RM-352: >31,000 ^{14}C yr bp (yr BP)[39]. The sample comprised a piece of charcoal recovered from layers E II-I excavated in 1966.

More recently, four new radiocarbon determinations (AA-66812: 34,900 ± 1900 yr BP, AA-66813: 32,300 ± 2700 yr BP, AA-66814: 36,510 ± 2300 yr BP, AA-66819: 36,600 ± 2300 yr BP) were reported by Ronchitelli et al.[47] and Kuhn et al.[48]. They belong to a series of ten AMS dates made on burnt bone from layer E III ranging from 21,000–36,000 yr BP with no age-depth consistency[49]. This is not surprising because burnt bone is an unreliable material for AMS dating[50]. It consists of pyrolysed collagen, often with sediment carbon and non-autochthonous material within it, and has a tendency to produce ages that often underestimate the true age, especially of Palaeolithic-aged samples.

These previous dates, therefore, can only serve as a minimum estimate of the real age of layer EIII, and should be set to one side.

New radiocarbon chronology

Material

More recent chronometric work has been undertaken by one of us (KD) as part of a D.Phil project at the University of Oxford[51], supervised by Prof. R.E.M. Hedges. Two shells from the uppermost layers D II and D I of the original 1963 excavations[31] were selected for dating from the *Soprintendenza per i Beni Archeologici della Puglia* in Taranto. In addition, six shells from the salvage fieldwork in the 1970s and 1980s were sampled from the collection housed at the University of Siena. All dated shells are shown in Fig. S3.

The *Dentalium* sp. shells (Cvl 3, 4, 5, 8, 11) are of smooth morphology and have been snapped transversely to create regular tube-shaped beads. The *Nuculana* sp. shell (Cvl 2) is a relatively uncommon species in Upper Palaeolithic ornamental assemblages and was one of eight similarly perforated small valves from the same context.

Pretreatment methods

All new radiocarbon dates in this paper were produced at the Oxford Radiocarbon Accelerator Unit (ORAU), University of Oxford. Ten determinations were obtained from eight shells –Cvl 10 and 5 were dated twice for methodological reasons or as internal laboratory checks.

Part of each shell was cleaned using an air-abrasive system with aluminum oxide until the surface was removed and the inner shell structure was exposed. A small fragment of the carbonate was sawn off and crushed in an agate mortar and pestle to a fine powder. Approximately 30mg of powdered sample was reacted with 5ml of 80% phosphoric acid (H_3PO_4) for 12h at 60^{o}C, under vacuum. The CO_2 evolved via this process was extracted through a manifold and cryogenically purified while passing through a liquid N_2–methanol cooled trap that removes less volatile impurities (H_2O and phosphoric acid vapour). The gas was injected through an automated elemental analyzer connected to a continuous flow isotope-ratio-monitoring mass spectrometer (EA-CF-IRMS) system where it was measured isotopically. The CO_2 remaining from the process was transferred to a graphitization rig and was reduced to graphite with H_2 at 560 °C for 6h, in the presence of ≈2 mg of a Fe^+ catalyst. The graphite was pressed into a target holder prior to accelerator mass spectrometry (AMS).

Results

The raw determinations and sample details are given in Table S5. The majority of the new radiocarbon dates (OxA-19242, OxA-19256, OxA-19258, OxA-20631, OxA-19255, OxA-19254) are consistent with respect to the stratigraphic position of the samples.

Only OxA-19257 from horizon D II is too old for its context. This is *not* an ornament but a small, indeterminate fragment of a bivalve shell (Fig. S3; Cvl 6). Its preservation state was poor and the sample surface showed alteration and a chalky appearance. Given that the rest of the shells are much better preserved and with a very low degree of fragmentation a possible

explanation may be that Cvl 6 is an old shell, either collected on purpose, or accidentally brought to the site. Bivalve shells are found in lower layers of Cavallo and the breaking pattern, the small dimensions and the old age of Cvl 6, in contrast with the rest of the shell Uluzzian assemblage, supports the suggestion of an old or redeposited specimen.

In contrast, OxA-21072 (and its duplicate) was obtained from a *Cyclope neritea* shell, discovered during the original excavation of Palma di Cesnola in 1963 in layer D I on the top of the Uluzzian sequence. The material was stored in Taranto since the 1960s separately from the other dated samples. These dates are surprising young, especially since there has been no other archaeological material of a similar age discovered in Cavallo Cave.

Infiltration of younger Epigravettian material to the uppermost Uluzzian layer D I would require passing through the stalagmitic crust and the volcanic ash layers (see Fig. S1). However, according to the excavator's observations the ash and the stalagmite crust formed a continuous layer. While we suspect several reasons might be responsible for this younger age, we cannot prove them. What is certain, however, is that the sample does not truly relate to the Uluzzian layers. Other similarly young material has not been discovered in the Uluzzian layers and the few Aurignacian-like elements observed at the uppermost Uluzzian layer D I were considered by Palma di Cesnola to belong to a transitional, Terminal Uluzzian phase, before the arrival of the Protoaurignacian in the region[40].

XRD analyses

Prior to chemical pretreatment, all samples were mineralogically characterized using X-Ray Diffraction (XRD), following the optimized methods described by Douka et al.[52] which allow detection and quantification of very low amounts of calcite in binary mixtures with aragonite. With the exception of Cvl 3, all shells appeared well-preserved and largely unaffected by

diagenesis (Table S5 shows the percentage of calcite present in the naturally aragonitic shell samples).

Cvl 3 contained large amounts of calcite (≈50%) in the originally aragonite structure. The sample was examined microscopically and no evidence of mineral overgrowth or other form of alteration was observed. It is very likely that the formation of calcite was caused by exposure to high temperature (over 230^{o}C) which readily alters biogenic aragonite to calcite. This would not incorporate a shift in the radiocarbon age. OxA-19242 is in very good agreement with the rest of the dates from overlying spits of layers E and D (see below).

Cvl 5 was also dated twice as part of an experimental project where the effect of surface cleaning (by abrasion) was examined. The results of the two methods are statistically indistinguishable, but the first determination (OxA-19256) is preferred over the second date (OxA-X-2280-16), given that the fraction used for the latter was not thoroughly cleaned.

Bayesian model

In an attempt to place the two human teeth, Cavallo-B and Cavallo-C, within their most likely age and palaeoclimatic context, the new radiocarbon determinations were incorporated into a Bayesian model built with OxCal 4.1.7[53] and calibrated using the INTCAL Marine09 curve[54]. This is an interim curve and will be refined as additional datasets become available and are incorporated into it.

The Bayesian model (Fig. S4) includes prior stratigraphic information as observed at the site during excavation, as well as the presence of the tephra on top of the Uluzzian sequence, here taken as the CI (≈39,300 ± 55 yr BP)[55]. This age estimate has been produced from an average of 36 ^{40}Ar/^{39}Ar measurements from twelve proximal deposits. Since there is no chemical identification of the tephra capping the Uluzzian deposits in Cavallo, the probability distribution for the CI is only tentatively placed on top of the Bayesian plot. An outlier

detection analysis was used to assess outliers in the model. This showed two outliers of significance: OxA-21072 and its duplicate date (not shown in Fig. S4) and OxA-19257.

The earliest Uluzzian phase of layer E III, in which Cavallo-B was found, was not dated directly due to the lack of suitable samples. Using the `Date` function in OxCal, however, we calculated a probability distribution function (PDF) for the likely age of the human fossil within this phase. This PDF corresponds to a range between 45,010—43,380 (68.2% prob.) and 47,530—43,000 (95.4% prob.) cal yr BP with respect to INTCAL Marine09 (Fig. S5). The longer tail of the distribution and wider uncertainty is caused because it is unconstrained by chronometric data below the Uluzzian layers. Further work is needed to refine this estimate for the age of the layer.

The oldest radiocarbon determination from the site comes from E II-I and places the evolved Uluzzian –and the age of Cavallo-C– at about 40,000 ^{14}C yr BP or 43,000 cal yr BP. This date also acts a *terminus ante quem* for Cavallo-B and the arrival of modern humans in the cave. The PDF for the age of Cavallo B determined using the `Date` function in OxCal ranges between 43,970—43,060 (68.2% prob.) and 44,910—42,660 (95.4% prob.) cal yr BP.

The two age estimates overlap significantly, although the PDF for EIII is by definition older than that of EII-I (Fig. S5).

We compare these data tentatively against the NGRIP δ^{18}O record[56,57] tuned with respect to the Hulu Cave U-series chronology (following Weninger and Jöris[58]) (Figs. S4, S5). The PDF for EIII fits within the latter part of GIS 12 on this timescale, while the PDF for EII-I is slightly later (Fig. S5). Overall, the radiocarbon determinations from Grotta del Cavallo agree with the stratigraphic position of the majority of the samples and the presence of the CI ash. This is the first time the Uluzzian of the type-site of Grotta del Cavallo has been dated reliably since its discovery in 1963.

Confirmation of the age of the La Rochette and Brillenhohle specimens

We checked the age of these two comparative human specimens by redating the samples to confirm their antiquity (Table S6).

Supplementary Figures

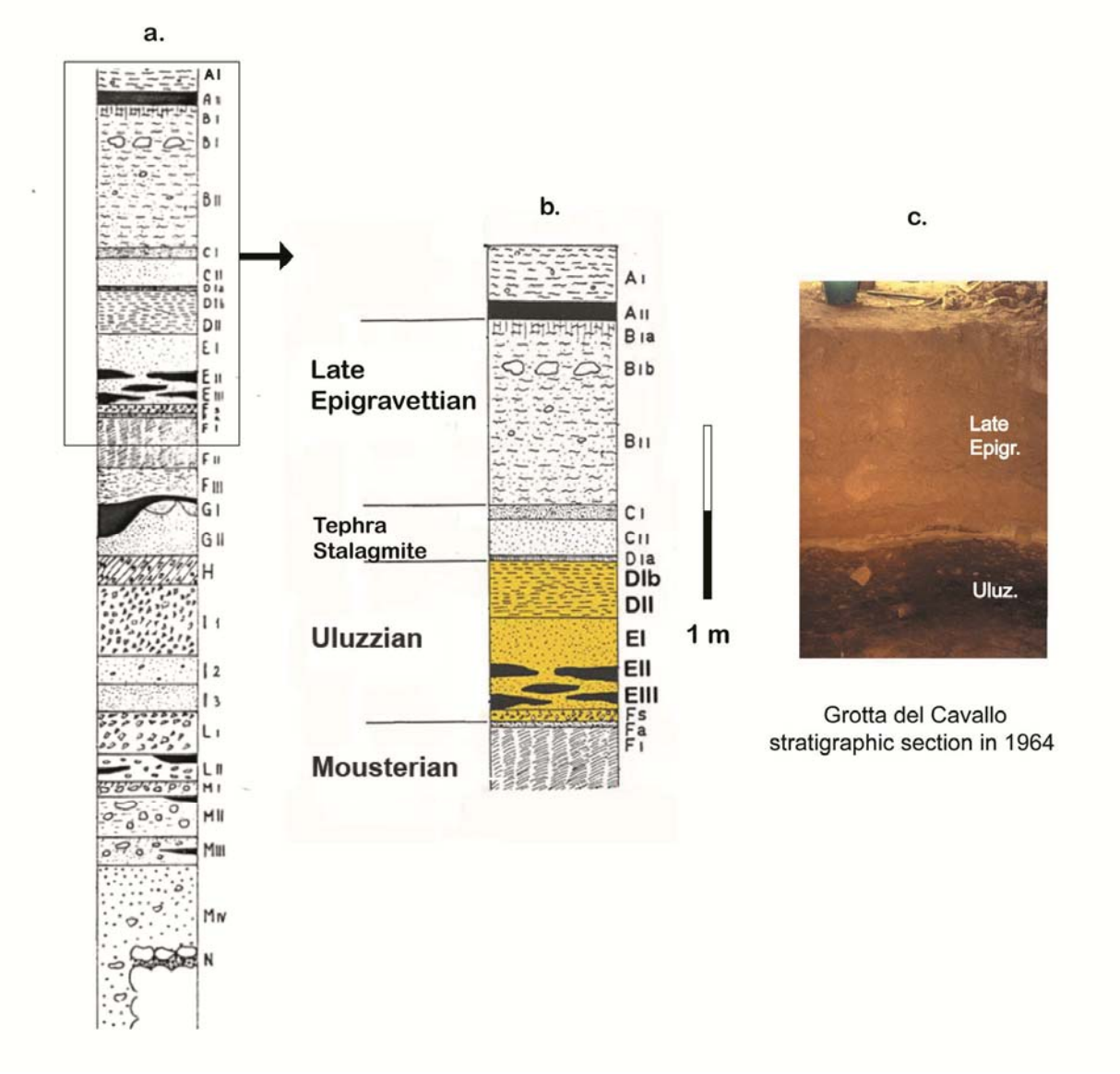

Figure S1: Section drawing of the Palaeolithic sequence of Grotta del Cavallo. **a**, The entire stratigraphic section of Cavallo Cave, after Palma di Cesnola[38]; **b**, detail of the section showing only the late Mousterian and UP layers; **c**, the section photograph illustrates the clear distinction between the very dark Uluzzian deposits from the lighter-coloured sediments of the later UP layers at the site.

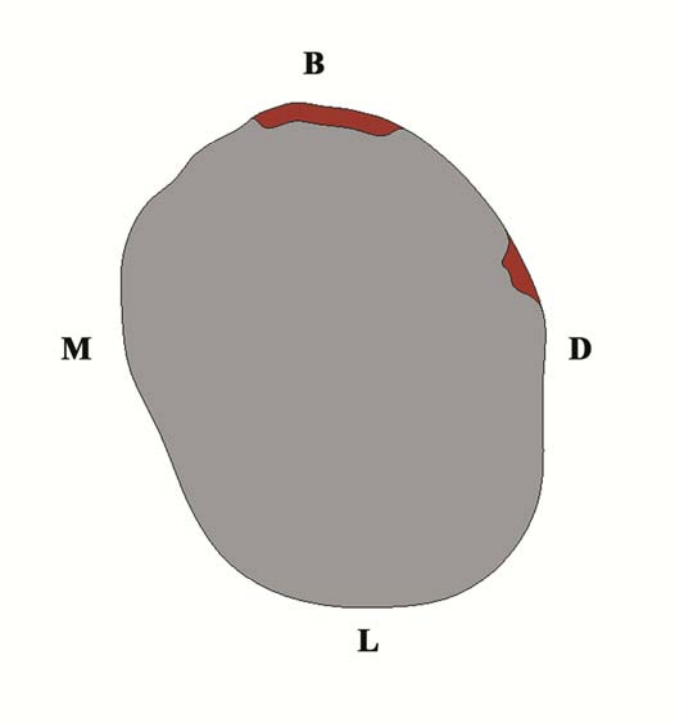

Figure S2: 2D virtual reconstruction of Engis 2 dM^1 crown outline. The crown outline of the original tooth is in grey; the reconstructed portions are shown in red. B=buccal; D=distal; L=lingual; M=mesial.

Figure S3: **Marine shells from the Uluzzian layers of Grotta del Cavallo used for AMS dating**. *Dentalium* sp. (Cvl 3, 4, 5, 8, 11), *Nuculana* sp. (Cvl 2), *Cyclope neritea* (Cvl 10) and bivalve fragment (Cvl 6).

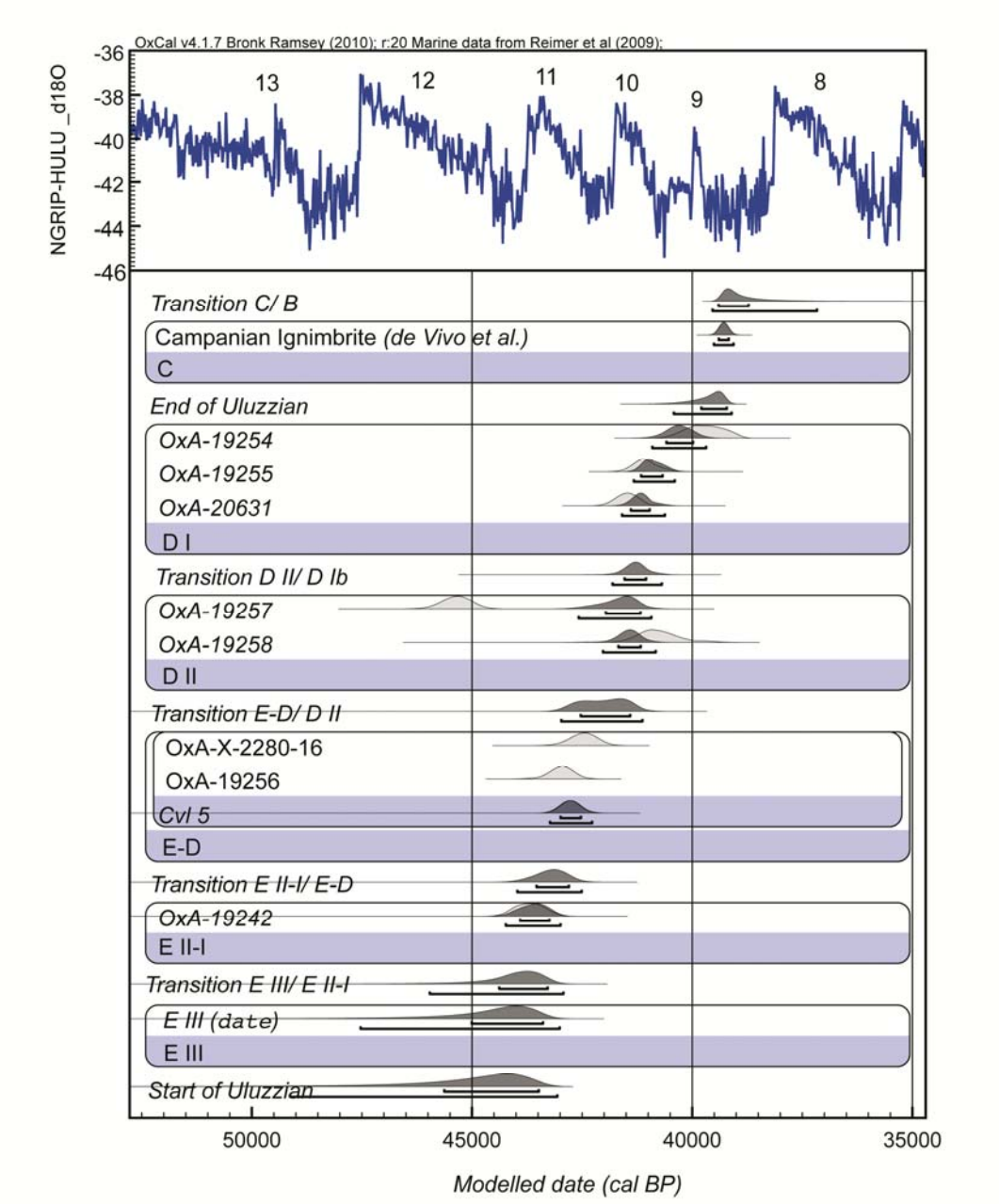

Figure S4: Bayesian model of the calibrated radiocarbon dates obtained on shell material from the Uluzzian layers of Cavallo. The radiocarbon dates are calibrated using the INTCAL Marine09 curve[54] with resolution set at 20. The NGRIP $\delta^{18}O$ record is shown[56,57] tuned with the U/Th chronology for the Hulu Cave speleothem[58]. Individual likelihoods are shown with lighter shaded distributions. Posterior probability distributions are in black outline. OxA-19257 is an outlier (100% chances for being an outlier) and most probably corresponds to an 'old' or redeposited shell (see text). The rest of the determinations demonstrate a consistent trend of decreasing age until the time of the inferred CI eruption.

OxA-19254 is in perfect agreement with this age. The very young dates from Cvl 10 (OxA-21072 and duplicate) are not included in the figure since they certainly do not relate to the Uluzzian occupation (see text). Cvl 5 was dated twice. Figure generated using OxCal 4.1.7[53].

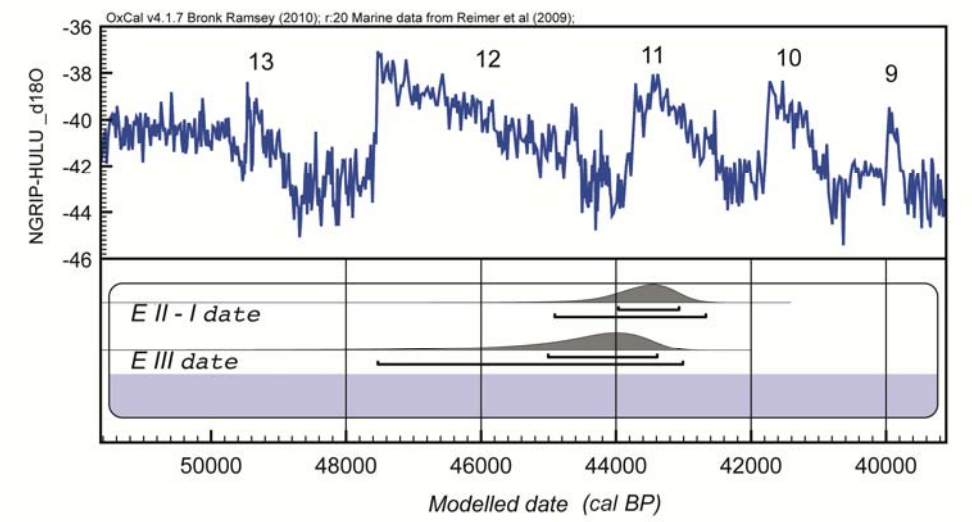

Figure S5: Age estimates for the human remains found in Cavallo layers **EIII and EII-I.** These ages are `Date` estimates, no direct measurements, which provide probability distribution functions (PDFs) for the likely age for the human teeth in layers EIII and EII-I. The NGRIP $\delta^{18}O$ record is shown[56,57], tuned with respect to the U/Th chronology for the Hulu Cave speleothem[58]. The relevant Greenland interstadials (GI) are given. Figure generated using OxCal 4.1.7[53].

Supplementary Tables

Table S1: Cross-correlation of Uluzzian layers at Cavallo, revealed in the original excavations of Palma di Cesnola (1963-1966) and in the subsequent rescue operations in the late 1970s and early 1980s.

Layers (1963-1966)	Spits (1978-1984)
DIb	D1–D2
DII	D3–D4
E-D	E 1
EII-I	E2–E4
EIII	E5–E7

Table S2: List of Neanderthal (N) and modern human (UPMH and RMH) dM^1s and dM^2s

	dM^1				dM^2			
Taxon	Specimen	Country	Source	Wear stage[d]	Specimen	Country	Source	Wear stage[d]
N	Engis 2[e]	Belgium	NESPOS[a]	stage 4	Krapina d185	Croatia	NESPOS[a]	unworn
	Krapina d181	Croatia	NESPOS[a]	stage 3	Krapina d186	Croatia	NESPOS[a]	unworn
	Krapina d183	Croatia	NESPOS[a]	stage 3	Krapina d187[g]	Croatia	NESPOS[a]	stage 3
	Pech-de-l'Azé I-R	France	Original data	stage 3	Krapina d188	Croatia	NESPOS[a]	unworn
	Pech-de-l'Azé I-L	France	Original data	stage 3	Krapina d189[g]	Croatia	NESPOS[a]	stage 3
	Roc de Marsal 1-R	France	NESPOS[a]	stage 3	Krapina d190	Croatia	NESPOS[a]	stage 1
	Roc de Marsal 1-L	France	NESPOS[a]	stage 3	Pech-de-l'Azé I-R	France	Original data	stage 1
	Subalyuk 2-R[e]	Hungary	Original data	stage 3	Pech-de-l'Azé I-L	France	Original data	stage 1
					Roc de Marsal 1-R	France	NESPOS[a]	unworn
					Roc de Marsal 1-L	France	NESPOS[a]	unworn
					Subalyuk 2-L	Hungary	Original data	stage 1
UPMH[b]	Brillenhöhle[f]	Germany	Original data	stage 3	Dolni Vestonice 36-3	Czech Republic	Original data	stage 1
	Dolni Vestonice 36-2	Czech Republic	Original data	unworn	La Rochette	France	Original data	stage 2
	La Rochette	France	Original data	stage 3	Pavlov 6[g]	Czech Republic	Original data	stage 4
					Pavlov 12[g]	Czech Republic	Original data	stage 6
RMH[c]	From Medieval and contemporary samples	France: 2 Germany: 11 Italy: 9	Original data	Unworn: 5 Stage 1: 3 Stage 2: 0 Stage 3: 14	From Medieval and contemporary samples	France: 2 Germany: 10 Italy: 11	Original data	Unworn: 5 Stage 1: 9 Stage 2: 6 Stage 3: 3

[a]NESPOS Database 2011/ www.nespos.org/display/openspace/Home; [b]UPMH= Upper Paleolithic modern human; [c]RMH= recent modern human; [d]based on Smith[42]; [e]used only for crown outline analysis; [f]used only for 2D enamel thickness and dental tissue proportions; [g]used only for cervical outline analysis

Table S3: 2D enamel thickness of Cavallo-B and Cavallo-C compared with Neanderthal (N), Upper Paleolithic modern human (UPMH), recent modern human (RMH) dM^1s and dM^2s (SD in brackets)

Tooth	Taxon	Wear stage[a]	n	Enamel area (mm^2)	Coronal dentine area (mm^2)	EDJ[b] length (mm)	AET[c] (mm)	RET[d] (scale free)
dM^1	N	3	6	7.02 (0.69)	31.76 (2.10)	17.36 (0.42)	0.40 (0.03)	7.17 (0.54)
	UPMH	3	2	7.26 (1.10)	28.16 (0.84)	14.28 (1.75)	0.51 (0.01)	9.56 (0.13)
	RMH	3	12	7.28 (0.65)	26.62 (1.51)	15.38 (0.78)	0.47 (0.03)	9.19 (0.70)
	UPMH	unworn	1	9.63	29.14	17.22	0.56	10.36
	RMH	unworn-stage 1	8	8.39 (1.26)	26.18 (1.73)	16.39 (0.73)	0.51 (0.06)	9.96 (0.96)
	Cavallo-B	unworn		12.64	34.14	18.33	0.69	11.80
dM^2	N	unworn-stage 1	9	12.14 (1.23)	33.85 (5.10)	19.25 (1.39)	0.63 (0.04)	10.89 (0.84)
	UPMH	stage 1-stage 2	2	16.75 (3.14)	28.93 (4.23)	17.30 (0.64)	0.97 (0.15)	17.93 (1.40)
	RMH	unworn-stage 3	20	12.33 (1.61)	28.36 (2.32)	16.83 (0.93)	0.73 (0.09)	13.78 (1.63)
	Cavallo-C	stage 5		13.4	34.59	15.96	0.84	14.28

[a]Based on Smith[42]; [b]EDJ= enamel-dentine junction; [c]AET = average enamel thickness index; [d]RET = relative enamel thickness index

Table S4: Summary of the leave-one-out cross validation Quadratic Discriminant Analysis (QDA)

Tooth	Parameter	n	Classified $P_{post} \geq 0.90$ MH	Classified $P_{post} \geq 0.90$ N	Indetermined $0.10 < P_{post} < 0.90$	Missclassified $P_{post} \geq 0.90$	Taxa %	Accuracy %
dM^1	Outline	32	20 (24)	7 (8)	5	1	84.4	96.3
	RET	31	23 (24)	4 (7)	4	0	87.1	100
	AET	31	14 (24)	3 (7)	14	0	54.8	100
	Cavallo-B		$P_{post} = 0.98$[a]					100[c]
dM^2	Outline	38	25 (27)	11 (11)	2	0	94.7	100
	RET	34	21 (25)	7 (9)	6	0	82.3	100
	AET	34	13 (25)	0 (9)	21	0	38.2	100
	Cavallo-C		$P_{post} = 0.99$[a]					100[c]
			$P_{post} = 0.99$[b]					100[c]

P_{post} = posterior probability; n = sample size; () = original group sample size; MH = modern human (UPMH and RMH); N = Neanderthal. AET = average enamel thickness index; RET = relative enamel thickness index; Species % = percentage of specimens for which a taxon is determined with $P_{post} \geq 0.90$ after cross validation; Accuracy % = percentage of specimens correctly classified after cross-validation; [a] P_{post} based on outline data; [b] P_{post} based on RET data; [c] Percentage of iterations (during cross validation) for which Cavallo's tooth is classified as modern human with a $P_{post} \geq 0.90$.

Table S5: New radiocarbon determinations for the Uluzzian layers in Grotta del Cavallo

Sample	OxA	^{14}C yr BP	±	Layer-Spit	Species	Calibrated (95.4%) yr BP from	Calibrated (95.4%) yr BP to	Aragonite-Calcite %
Cvl 10	21072	19,685	75	D I	*Cyclope neritea*	23,380	22,470	100-0
Cvl 10	Dupl.	19,235	75	D I	*Cyclope neritea*	23,220	22,060	100-0
Cvl 2	19254	35,080	230	D 1=DIb	*Nuculana* sp.?	40,450	38,860	100-0
Cvl 4	19255	36,260	250	D 2=DIb	*Dentalium* sp.	41,570	40,390	100-0
Cvl 11	20631	36,780	310	D II	*Dentalium* sp.	42,010	40,880	99.8-0.2
Cvl 6	19257	42,360	400	D 3=D II	Bivalve fragm.	45,990	44,640	100-0
Cvl 8	19258	36,000	400	D 8=DII?	*Dentalium* sp.	41,570	39,560	100-0
Cvl 5	19256	39,060	310	E 1=E-D	*Dentalium* sp.	43,510	42,350	99.7-0.3
Cvl 5	X-2280-16	38,300	400	E 1=E-D	*Dentalium* sp.	43,380	42,080	100-0
Cvl 3	19242	39,990	340	E 4=EII-I	*Dentalium* sp.	44,300	43,000	50-50

Conventional ages are expressed in ^{14}C years BP, after Stuiver and Polach[59]. Note that layer assignation for Cvl 10 and Cvl 11 follows that of the original excavations[31]. The rest of the shells were recovered during rescue excavations in subsequent years and follow different assignation system. The correlation of the two series is based on field documentation. Percentages of aragonite to calcite are listed in the right hand column based on high precision XRD analysis.

Table S6: Radiocarbon determinations from La Rochette and Brillenhöhle

Specimen	OxA	^{14}C yr BP	±	Used (mg)	Yield (mg)	%Yld	%C	$d^{13}C$ (‰)	$d^{15}N$ (‰)	C:N atomic ratio
La Rochette	11053	23,630	130	710	34.2	4.8	45.8	-17.1	11.7	3.3
	23413	23,400	110	na	23.84	3.4	42.9	-17.2	11.9	3.1
Brillenhöhle	11054	12,470	65	600	34.7	5.8	44.7	-19.2	8.5	3.3
	23414	12,535	50	na	22.67	3.8	42.5	-19.5	8.5	3.1

Conventional ages are expressed in years BP, after Stuiver and Polach[59]. Stable isotope ratios are expressed in ‰ relative to vPDB with a mass spectrometric precision of ±0.2‰. Gelatin yield represents the weight of gelatin or ultrafiltered gelatin in milligrams. %Yld is the percent yield of extracted collagen as a function of the starting weight of the bone analysed. %C is the carbon present in the combusted gelatin. CN is the atomic ratio of carbon to nitrogen and is acceptable if it ranges between 2.9—3.5. The new AMS dates are reultrafiltered gelatin sample extracted from the first pretreatment chemistries undertaken. This was done as a check on the original filtration chemistry. You can see that the results are statistically identical and confirm the original measurements.

Supplementary References

31. Palma Di Cesnola, A. Prima campagna di scavi nella Grotta del Cavallo presso Santa Caterina (Lecce). *Riv. Sc. Preist.* **18**, 41-74 (1963).

32. Palma di Cesnola, A. Seconda campagna di scavo nella grotta del Cavallo. *Riv. Sc. Preist.* **19**, 23-39 (1964).

33. Palma di Cesnola, A. Notizie preliminari sulla terza campagna di scavi nella Grotta del Cavallo (Lecce). *Riv. Sc. Preist.* **20**, 291-302 (1965a).

34. Palma di Cesnola, A. Gli scavi nella Grotta del Cavallo (Lecce) durante il 1966. *Riv. Sc. Preist.* **21**, 289-302 (1966a).

35. Sarti, L., Boscato, P. & Lo Monaco, M. Il Musteriano finale di Grotta del Cavallo nel Salento, studio preliminare. *Origini* **22**, 45-109 (1998-2000).

36. Sarti, L., Boscato, P., Martini, F. & Spagnoletti, A.P. Il Musteriano di Grotta del Cavallo - strati H e I : studio preliminare. *Riv. Sc. Preist.* **52**, 21-110 (2002).

37. Palma di Cesnola, A. Il Paleolitico superiore arcaico (facies uluzziana della Grotta del Cavallo, Lecce. *Riv. Sc. Preist.* **20**, 33-62 (1965b).

38. Palma di Cesnola, A. Il Paleolitico superiore arcaico (facies uluzziana) della Grotta del Cavallo, Lecce (continuazione). *Riv. Sc. Preist.* **21**, 3-59 (1966b).

39. Palma di Cesnola, A. Datazione dell'Uluzziano col Metodo del C–14. *Riv. Sc. Preist.* **24**, 341–348 (1989).

40. Palma di Cesnola, A. *Il Paleolitico superiore in Italia* (Garlatti e Razzai, 1993).

41. Giaccio, B., Hajdas, I., Peresani, M., Fedele, F.G. & Isaia, R. in *When Neanderthals and Modern Humans Met* (ed. Conard, N.J.) (Kerns Verlag, Tubingen, 2006).

42. Smith, B.H. Patterns of molar wear in hunter-gatherers and agriculturists. Am. J. Phys.

Anthropol. 63, 39-56 (1984)

43. Spoor, F., Zonneveld, F. & Macho, G.A. Linear measurements of cortical bone and dental enamel by computed tomography: applications and problems. *Am. J. Phys. Anthropol.* **91**, 469-484 (1993).

44. R Development Core Team. R: a language and environment for statistical computing. Vienna, Austria: R Foundation for Statistical Computing.http://www.r-project.org. (2008).

45. Anderson, T.W. Asymptotic Theory for Principal Component Analysis. *Ann. Math. Statist.* **34**, 122-148 (1963).

46. Coquerelle, M. et al. Sexual dimorphism of the human mandible and its association with dental development. *Am. J. Phys. Anthropol.* **145**, 192-202 (2011).

47. Ronchitelli, A., Boscato, P. & Gambassini, P. in La lunga storia di Neandertal. Biologia e comportamento (eds Facchini, F. & Belcastro, G.M.) (Jaca Book, 2009).

48. Kuhn, S.L. et al. Radiocarbon Dating Results for the Early Upper Paleolithic of Klissoura 1 Cave. *Euras. Prehist*. 7 (2), 37-46 (2010).

49. Riel-Salvatore, J. The Uluzzian and the Middle-Upper Paleolithic Transition in Southern Italy. Unpublished Ph.D. dissertation, School of Human Evolution and Social Change, Arizona State University (2007).

50. Van Strydonck, M., Boudin, M. & De Mulder, G. ^{14}C dating of cremated bones: the issue of sample contamination. *Radiocarbon* **51**, 553-568 (2009).

51. Douka, K. *Investigating the Chronology of the Middle to Upper Palaeolithic Transition in Mediterranean Europe by Improved Radiocarbon Dating of Shell Ornaments*. Unpublished D.Phil in Archaeological Science, University of Oxford (2011).

52. Douka, K., Hedges, R.E.M., Higham, T.F.G., 2010. Improved AMS ^{14}C dating of shell

carbonates using high-precision X-Ray Diffraction (XRD) and a novel density separation protocol (CarDS). *Radiocarbon* 52 (2): 735–751.

53. Bronk Ramsey, C. Bayesian analysis of radiocarbon dates. *Radiocarbon* **51**, 337-360 (2009).

54. Reimer, P.J. *et al*. IntCal09 and Marine09 radiocarbon age calibration curves, 0–50,000 years cal BP. *Radiocarbon* **51**, 1111-1150 (2009).

55. De Vivo, B., Rolandi, G., Gans, P.B., Calvert, A., Bohrson, W.A., Spera, F.J. & Belkin, H.E. New constraints on the pyroclastic eruptive history of the Campanian volcanic Plain (Italy). *Mineral. Petrol.* **73**, 47–65 (2001).

56. Andersen, K.K. *et al*. The Greenland ice core chronology 2005, 15-42 ka. Part 1: constructing the time scale. *Quat. Sci. Rev.* **25**, 3246-3257 (2006).

57. Svensson, A. *et al*. The Greenland ice core chronology 2005, 15-42ka. Part 2: Comparison to other records. *Quat. Sci. Rev.* **25**, 3258-3267 (2006).

58. Weninger, B., Jöris, O. A ^{14}C age calibration curve for the last 60 ka: the Greenland-Hulu U/Th timescale and its impact on understanding the Middle to Upper Paleolithic transition in Western Eurasia. *Journal of Human Evolution* **55**, 772–781 (2008).

59. Stuiver, M. & Polach, H.A. Discussion: Reporting of ^{14}C Data. *Radiocarbon* **19**, 355-363 (1977).